Direct contact membrane distillation of refining waste stream from precious metal recovery: chemistry of silica and chromium (III) in membrane scaling

Gang Chen[1, 2], Lihua Tan[1, 2], Ming Xie[3], Yanbiao Liu[1, 2], Yanli Lin[4], Wenjin Tan[5], Manhong Huang[1, 2]*

[1]College of Environmental Science and Engineering, Donghua University, Shanghai 201620, China

[2]Textile Pollution Controlling Engineering Centre of Ministry of Environmental Protection, Shanghai 201620, China

[3]Department of Chemical Engineering, University of Bath, BA2 7AY, UK

[4]Shanghai justhave environmental engineering Co., Ltd., Shanghai, 201620, China

[5]Sino-Platinum metals resources (Yimen) Co., Ltd., Kunming 650106, China

Phone: +86-21-67792546; Fax: 0086-21-67792159; Email: huangmanhong@dhu.edu.cn

Abstract

Precious metals such as platinum group metals (PGMs) with distinct catalytic activity are widely used as active components in various industrial catalysts. It is, therefore, highly desirable to recover these valuable components from end-of-life products. We explored the treatment of refining wastewater from precious metals recovery using direct contact membrane distillation (DCMD). The role of various initial pH of refining wastewater on DCMD performance was assessed. Results suggest that hydrochloride acid (HCl) and high-quality water can be reclaimed from the real refining wastewater by adjusting initial pH. Furthermore, DCMD water flux decline was mainly caused by silica and chromium (III) scaling, which was dependent on initial pH of refining wastewater. Silica scaling was responsible for the decrease of DCMD performance when the initial pH of refining wastewater shifted from original 0.03 to 5 and 7. Silica oligomers in the concentrated feed with various initial pH were identified using mass spectra. Whereas chromium (III) scaling was discovered, resulting in the used polytetrafluoroethylene (PTFE) membrane surface in green when the initial pH of refining wastewater was 3. Dichlorotetraaquochromiun, $[Cr(H_2O)_4Cl_2]Cl{\cdot}2H_2O$ was identified by X-ray photoelectron spectroscopy and ultraviolet and visible absorbance spectra as the main species contributing to the green colour of the scaled PTFE membrane surface. Our results suggest that DCMD can be used as a promising and feasible solution for resource recovery from acidic refining waste stream.

Keywords: precious metal recovery; refining wastewater; membrane distillation; silica and chromium (III) scaling

1. Introduction

Precious metals such as platinum group metals (PGMs) are widely used as the active components of various industrial catalysts due to their distinct catalytic activity, chemical inertness, corrosion resistance and thermoelectric stability, which were considered as "*Vitamin of modern industry*" [1-5]. The loading of precious metals in catalysts ranged from 0.02 to 100% [1]. The most significant applications of precious metals are electronics and catalystic industry, consuming over 90% of precious metals [2]. It was reported that about 65% of palladium (Pd, 182.65 tons), 45% of platinum (Pt, 98 tons) and 84% of rhodium (Rh, 25.6 tons) were used in catalytic converters [1, 2].

However, the global reserve of PGMs is only 66,000 tons and their reserve in Earth's crust is extremely low. For instance, In China, natural PGMs resources are extremely limited with total reserve of only about 350 tons. Only less than three tons of PGMs were mined in China annually, but demands for Pt and Pd were over 141 tons. Therefore, there is urgent demand to recycle these precious metals from end-of-life products to realize the sustainable development of precious metals [6, 7]. By 2016, about 30% of PGMs were recovered from spent catalysts, namely 34 tons of Pt, 61 tons of Pd and 7.2 tons of Rh. Precious metals in the spent catalysts are often leached in hydrochloric acid medium with oxidizing agents like HNO_3, Cl_2, NaClO, $NaClO_3$, H_2O_2, etc. through hydrometallurgical process [1, 8-10]. Besides precious metals, spent catalysts also contain many heavy metals [11]. Therefore, wastewater simultaneously generated from precious metals recovery process often contained high

66 concentrations of acids and various kinds of heavy metal ions, which has been
67 regarded as huge challenge [12]. From the perspective of resource recovery and
68 environmental protection, waste stream from precious recovery is crucial to be treated
69 before discharging into environment.

70 It has been reported that wastewater containing precious metals can be treated by
71 membrane filtration [13], electrochemical approach [14] and biosorption [15, 16]. For
72 example, forward osmosis (FO), an osmotically driven membrane technology, was
73 widely used in treatment of various industry wastewater [17-23] and was also capable
74 of Pd accumulation from printed circuit board (PCB) plant wastewater using an
75 electroless nickel plating solution as draw solution [13]. In addition, microbial fuel
76 cell (MFC) as one kind of bioelectrochemical systems was also employed for
77 recovery of precious metals such as silver. High silver removal rate (83±0.7%) and
78 recovery (67.8±1%) efficiencies were achieved from MFC fed with silver laden
79 artificial wastewater (MFC-Ag) after 72 h operation. COD removal rate of MFC-Ag
80 was up to 82.7±1.5% [14]. Furthermore, biosorption with advantages of low cost and
81 high effectiveness at low concentrations and environmentally friendly nature has been
82 widely developed for the recovery of metals ions from aqueous and waste solutions. A
83 range of bioadsorbents, such as *Escherichia coli* [24, 25], *Shewanella oneidensis*
84 MR-1[26], *Enterococcus faecalis* [27], *Phomopsis sp.* XP-8 [28], *Enterobacter*
85 *cloacae SgZ-5T* [29], *Galdieria sulphurariaetc* [30] etc., have been reported towards
86 biorecover Pd (II), Pt and Au from synthetic solutions. However, it is noteworthy that
87 the majority of the studies above were focused on precious metals recovery or

accumulation from synthetic solutions. Till now, treatment of real wastewater derived from precious metals recovery has been not reported. Therefore, it is necessary to investigate the treatment of real wastewater generated from process of precious metals recovery. However, in economically undeveloped and remote area in China, the actual solution for removing heavy metal ions in the real wastewater derived from precious recovery was precipitation in alkali environment. This traditional physicochemical method not only increases cost of wastewater treatment but also produces large amount of physical and chemical sludge. Therefore, the dewatered sludge always contains various kinds of heavy metal ions and is a potential big threat to environment. In addition, China is a serious water shortage country, which is one of the 13 countries that lack of water all over the world [31]. From the perspective of water reclamation and environmental protection, if water reuse and heavy metal ions removal to an acceptable level is realized in application including industrial reuse, municipal green, and agricultural irrigation, which would have a great significant impact on cost reduction and decrease the negative influence on environment. An alternative technology that promises to achieve this objective is membrane distillation (MD).

Membrane distillation (MD) emerged as an advanced membrane technology was used to recover valuable salts [32, 33] as well as treatment of high salinity solution [34-36]. Compared with other membrane technologies such as reverse osmosis, MD possesses several advantages for brine minimization, such as low operating pressure, high water recovery, potential for 100% rejection of non-volatile solutes and small footprint [37]. However, it is well known that MD is a very energy intensive process.

To reduce or replace extra energy input, industrial waste heat and solar energy were used in MD process [38-40]. However, in the field of treatment of industrial waste stream via MD process, there was no report on the application of MD technology in treatment of the real wastewater generated from process of precious metals recovery. The aim of this work was to assess the treatment of the real refining wastewater with strong acidity from precious metals recovery through DCMD process. Effects of various initial pH of wastewater on DCMD performance and membrane scaling were systematically assessed. The changes of membrane surface color and morphology caused by silica and chromium (III) scaling under various pH values were recorded and interpreted, respectively. Various characterization techniques were employed to elucidate the underlying mechanisms of membrane scaling during the DCMD filtration.

2. Material and methods

2.1. MD membrane and wastewater

Commercial flat sheet MD membrane (PTFE-PVDF/PET) with mean pore size of 0.45 μm was purchased from Shanghai Minglie New Material Co., Ltd. The detail properties of commercial PTFE membrane were listed in Table S1. The structures of brine side facing feed solution and permeate side were shown in Fig. S1.

The real refining wastewater produced from the recovery of precious metals in spent catalysts was kindly provided by Sino-Platinum metals resources (Yimen) Co., Ltd. The key characteristic of the refining wastewater used is shown in Table 1. The refining wastewater is a clear yellow solution with a conductivity of 199.2 mS/cm and

initial pH of 0.03. Sodium and potassium ions are the major cations with concentrations of 11.36 g/L and 10.06 g/L, respectively. The major anion is chloride ion with concentration of 48.99 g/L.

Table 1 Key characteristic of refining wastewater used in this study

Analyzed items	Unit	Concentration
Conductivity	mS/cm	199.2 ± 1.4
pH	-	0.03 ± 0.02
COD	mg/L	3620 ± 200
Phosphate	mg/L	400 ± 80
Chloride	mg/L	48993.8 ± 1200.7
Nitrate	mg/L	1107.32 ± 50.82
Silicon	mg/L	11.92 ± 3.50
Sodium	mg/L	11364 ± 200
Potassium	mg/L	10058 ± 300
Zinc	mg/L	536.71 ± 8.75
Aluminum	mg/L	196.22 ± 3.05
Calcium	mg/L	64.07 ± 1.56
Iron	mg/L	46.50 ± 0.37
Magnesium	mg/L	36.80 ± 1.28
Copper	mg/L	14.46 ± 0.62
Chromium	mg/L	9.48 ± 1.13
Nickel	mg/L	6.27 ± 0.52

Manganese	mg/L	4.82 ± 0.21
Silver	mg/L	0.99 ± 0.12
Barium	mg/L	0.79 ± 0.15
Platinum	mg/L	0.57 ± 0.08

2.2. DCMD setup and experiments

A DCMD module made of transparent Perspex with a channel depth of 4 mm and effective area of 30 cm^2 (i.e. length 10 cm, width 3 cm) was used for experiments. Two same polyester spacers with diamond mesh were used to support the membrane and to promote the flow turbulence in both sides. The detail information of the module and spacer can be available in the previous report [34]. The schematic diagram and photo of the lab-scaled DCMD system used in this work is presented in Fig. S2 and Fig. S3 as reported previously [41-43]. The real refining wastewater with various initial pH was used as feed. Before experiments, feed and ultrapure water were put in the jacketed glass bottles with total volume of 1.5 liters, respectively. The effective volume of feed and ultrapure water was 1.2 and 1.5 liters for all experiments, respectively. Temperature of permeate side and brine side was maintained at 20±1°C and 60±1°C by circulating water cooler and thermostat circulating water bath, respectively. The flow rate for both sides was controlled at 300 mL/min (corresponding to the cross flow velocity of 8.3 cm/s) for all experiments by two same peristaltic pumps (Langer, BT600).

To investigate the influence of various initial pH of wastewater on MD performance, the initial pH of wastewater as the feed was adjusted from original 0.03 to 3, 5 and 7 using sodium hydroxide (23 wt%). Before experiments, the wastewater with various initial pH was first filtered by filter paper with mean pore size of 40 μm to remove visible species and then filtered again using 0.45 μm filter membrane to remove the small sized particles to maximally reduce membrane fouling during DCMD process. The permeate flux (J, kg/m^{2}h) was calculated by measuring the weight changes of permeate (Δm, kg)) with a precision balance (OHAUS, AR4202CN) divided by time intervals (Δt, h)) and membrane area (A, m^2), which was described in equation (1). Additionally, the conductivity of the accumulated permeate was online monitored by a conductivity meter (SUNTEX, EC-4110RS). Both the data of balance and conductivity meter was recorded by a computer equipped with a data logging system.

$$J = \frac{\Delta m}{\Delta t \cdot A} \qquad (1)$$

2.3. Analytical methods

Key element concentration of refining wastewater was determined with inductively coupled plasma-atomic emission spectroscopy (ICP-AES). The concentrations of chloride, phosphate and nitrate in refining wastewater were measured by ion chromatography (IC, LC20AT, Shimadzu, Japan). Field-emission scanning electron microscopy (FESEM, Hitachi S-4800) equipped with energy dispersive X-ray fluorescence spectrometer was used for analyzing the morphologies

of membranes and elementary composition of scalants. X-ray photoelectron spectroscopy (XPS) (Escalab 250Xi) was employed to analyze element chemical bonding. Fourier Transform Infrared Spectrometer (Nicoletln 10MX/Nicolet6700) was employed to analysis the ultraviolet and visible absorbance of the blank and scaled membrane surface. Electrospray ionization mass spectrometry (ESI-MS, Agilent 11000) was used to identify the silica oligomers formed in the concentrated solution with various initial pH. ESI negative ionization mode was used and the direct injection flow of the sample was 0.15 mL/min.

3. Results and discussion

3.1 DCMD performance

Fig. 1(A) shows the permeate flux patterns under various initial pH of refining wastewater. The curves of permeate flux displayed the similar trend, gradually decreased with the increasing of recovery. The initial flux for the original pH of 0.03 and 7 of refining wastewater were the same of 13 kg/m^{2}h, which is a little higher than that for pH of 3 and 5 also with same flux of 11.5 kg/m^{2}h. Then, the corresponding permeate flux for the initial pH of refining wastewater adjusted from original pH of 0.03 to 3, 5 and 7 declined to 8.4, 4.7, 4.6 and 5.9 kg/m^{2}h, respectively, when recovery reached to 60%. One reason for the decrease of fluxes is that feed solution concentrated and the partial vapor pressure of water in the feed solution decreased as increasing of recovery. Another reason is possibly that membrane scaling occurred under various initial pH of wastewater, which resulted in membrane scaling in varying

197 degree, thus caused various initial flux and flux at recovery of 60%. The changes of
198 permeate conductivity were depicted in Fig. 1(B). The permeate conductivity for
199 original pH of 0.03 and 3 increased exponentially, while the curves of permeate
200 conductivity for pH of 5 and 7 were much smoother. It was found amazingly that the
201 permeate conductivity increased from initial 7.6 μS/cm to 18.3 mS/cm when recovery
202 reached to 67% for the wastewater with original pH of 0.03. However, for the
203 wastewater with initial pH of 3, 5 and 7, the corresponding final permeate
204 conductivity was 338, 57.5 and 31.5 μS/cm, when the recovery went up to 66%, 60%
205 and 60%, respectively. These results indicated that high-quality permeate can be
206 reclaimed by controlling initial pH of feed solution. However, it is noteworthy that the
207 permeate conductivity for the pH of 3 spiked after recovery of 60%, indicating that
208 the PTFE membrane was possibly wet.

209 The pH values of the solution in permeate and feed tanks were also tested before
210 and after experiments. As shown in Fig. 2, compared with ultrapure water with
211 original pH of 5.46 in the permeate tank, the pH of the solution in the permeate tank
212 after experiment first decreased from 5.46 to 1.31 and 3.41, then increased to 6.45 and
213 7.2 as the initial pH of wastewater as feed shifted from original 0.03 to 3, 5 and 7,
214 respectively. In order to reveal the reason for the pH changes, water quality of the
215 solution in the permeate tank after experiment was characterized when original
216 refining wastewater was used as feed. The majority of anion is chloride ions (Cl^-) with
217 concentration of 545 mg/L and only small amount of cations such as Ca^{2+} (4.78 mg/L),
218 K^+ (0.38 mg/L), Na^+ (0.36 mg/L), Mg^{2+} (0.56 mg/L) coexists in the permeate (Table

2). It can be concluded from the data in Table 2 that the permeate for wastewater with original pH of 0.03 mainly consisted of hydrochloric acid (HCl). The reason for collection of HCl from waste stream with pH of 0.03 via DCMD process is possibly that under feed temperature of 60°C, the partial pressure of HCl over aqueous solution increased, resulting in Henry's law constant of HCl increase and solubility of HCl decline. Therefore, during DCMD filtration of wastewater with original pH of 0.03, HCl fast volatilized from feed solution with temperature of 60°C and passed through PTFE membrane into permeate, which resulted in permeate conductivity fast increased (Fig 1 B). These results above indicated that refining wastewater can be well treated as well as recovery of hydrochloric acid and high-quality water via DCMD process through adjusting initial pH of wastewater.

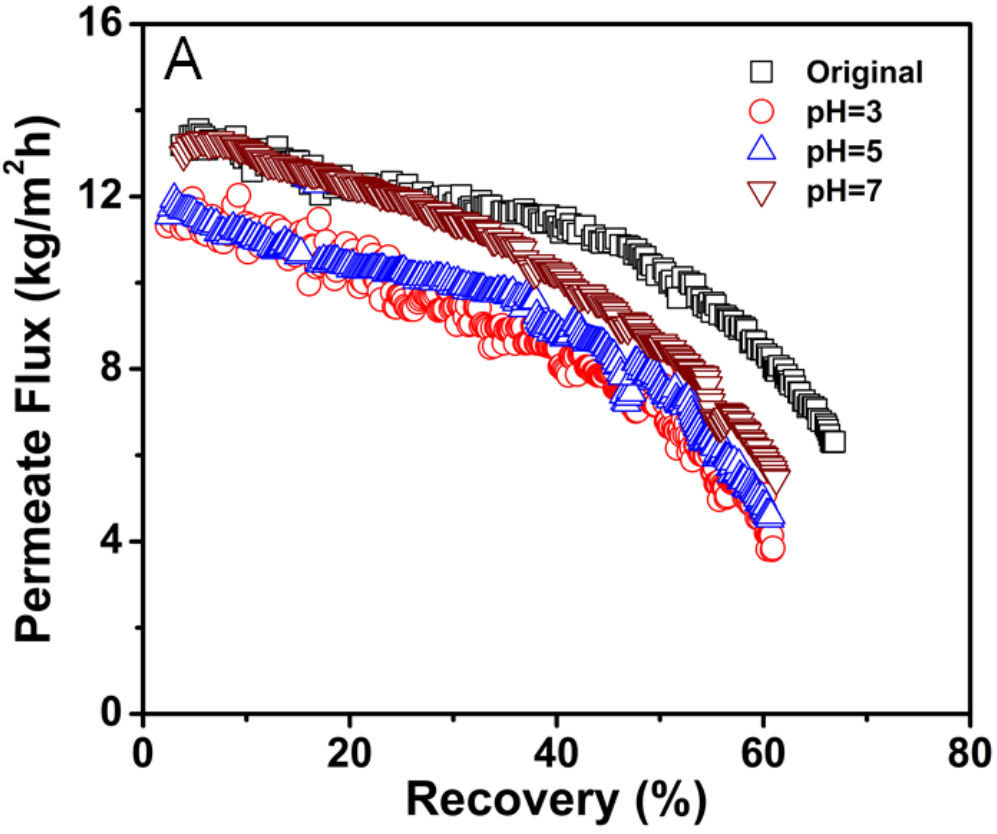

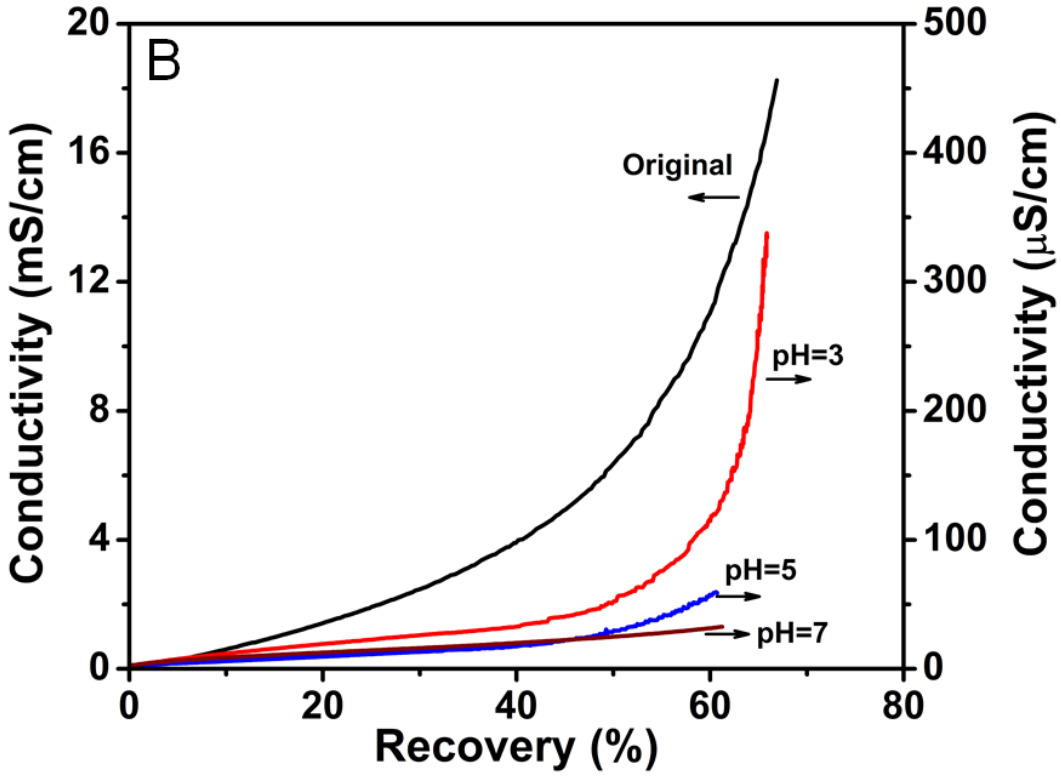

231

232 **Fig. 1.** DCMD experiment performance, permeate flux (A) and conductivity (B) as a

233 function of recovery for refining wastewater (Temperature of feed side and permeate

234 side was maintained at 60±1°C and 20±1°C, respectively; both the volumetric flow

235 rates of feed and permeate were controlled at 300 mL/min; the sodium hydroxide with

236 concentration of 23 wt% was used to adjust the feed pH).

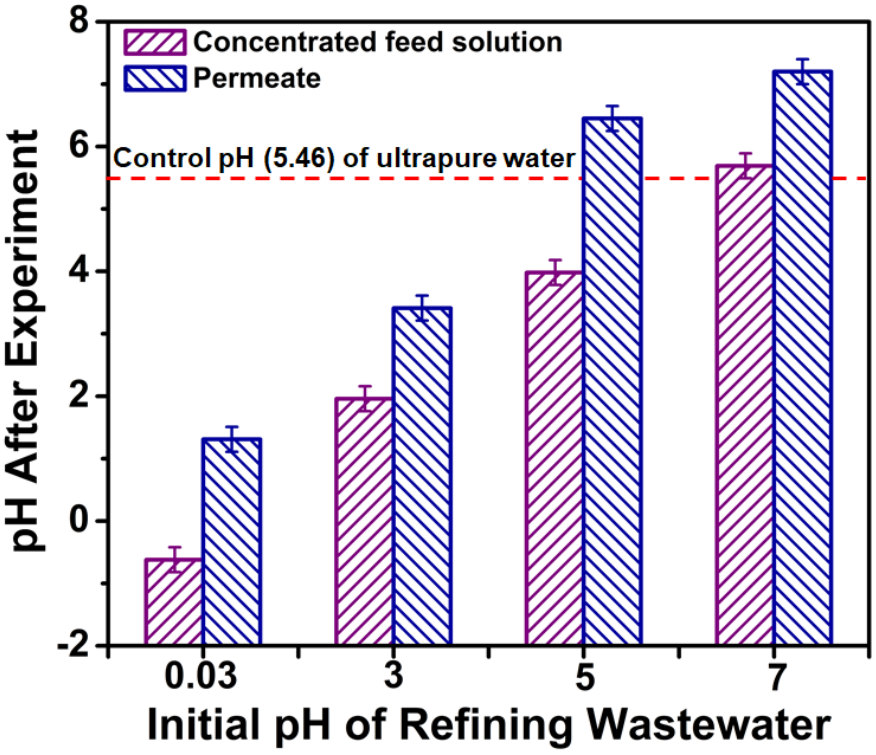

Fig. 2 pH changes of concentrated feed solution and permeate after experiments under various initial pH of wastewater as feed.

Table 2 Water quality of permeate from DCMD process using original refining wastewater as feed.

Analytes	Concentration (mg/L)
Chloride	545 ± 10
Potassium	0.38 ± 0.08
Sodium	0.36 ± 0.05
Calcium	4.78 ± 0.22
Magnesium	0.56 ± 0.13

3.2 Membrane surface color and contact angle

The colour of membrane surface facing feed has not changed significantly before and after experiments and was still white when the initial pH of the feed was adjusted from original 0.03 to 5 and 7 (Fig. 3). However, significant derivation of membrane surface colour was observed under the condition of wastewater as feed with initial pH of 3. As shown in Fig. 3, the membrane surface facing the feed and the permeate side of membrane facing cold side were both green, which was unexpected. Furthermore, the permeate side of membrane was more green than that of the brine side of membrane, meant that the greenish scalant possibly penetrated into membrane surface. This phenomenon was interpreted and the greenish scalant was identified in the following sections.

The contact angles of the brine side of PTFE membrane after experiments were shown in Fig. 4. For the refining wastewater with original pH of 0.03, the contact angle of PTFE membrane surface decreased from 112° to 72°, which provided clear evidence that the PTFE membrane surface after usage was partially wet. In contrary, the contact angle increased a little to 116° when the initial pH of the feed solution shifted to 7. However, for the refining wastewater with initial pH of 3 and 5, it was found that the contact angles of PTFE membrane surface were not obtained due to water droplet spreading, resulted from membrane wetting. These results indicated that the brine side of PTFE membrane surface after treatment of the real refining wastewater with initial pH of 3 and 5 were thoroughly wet. The phenomenon of contact angle changes was possibly related to the change of membrane surface morphologies and scalants deposited on membrane surfaces, which was observed as

267 below.

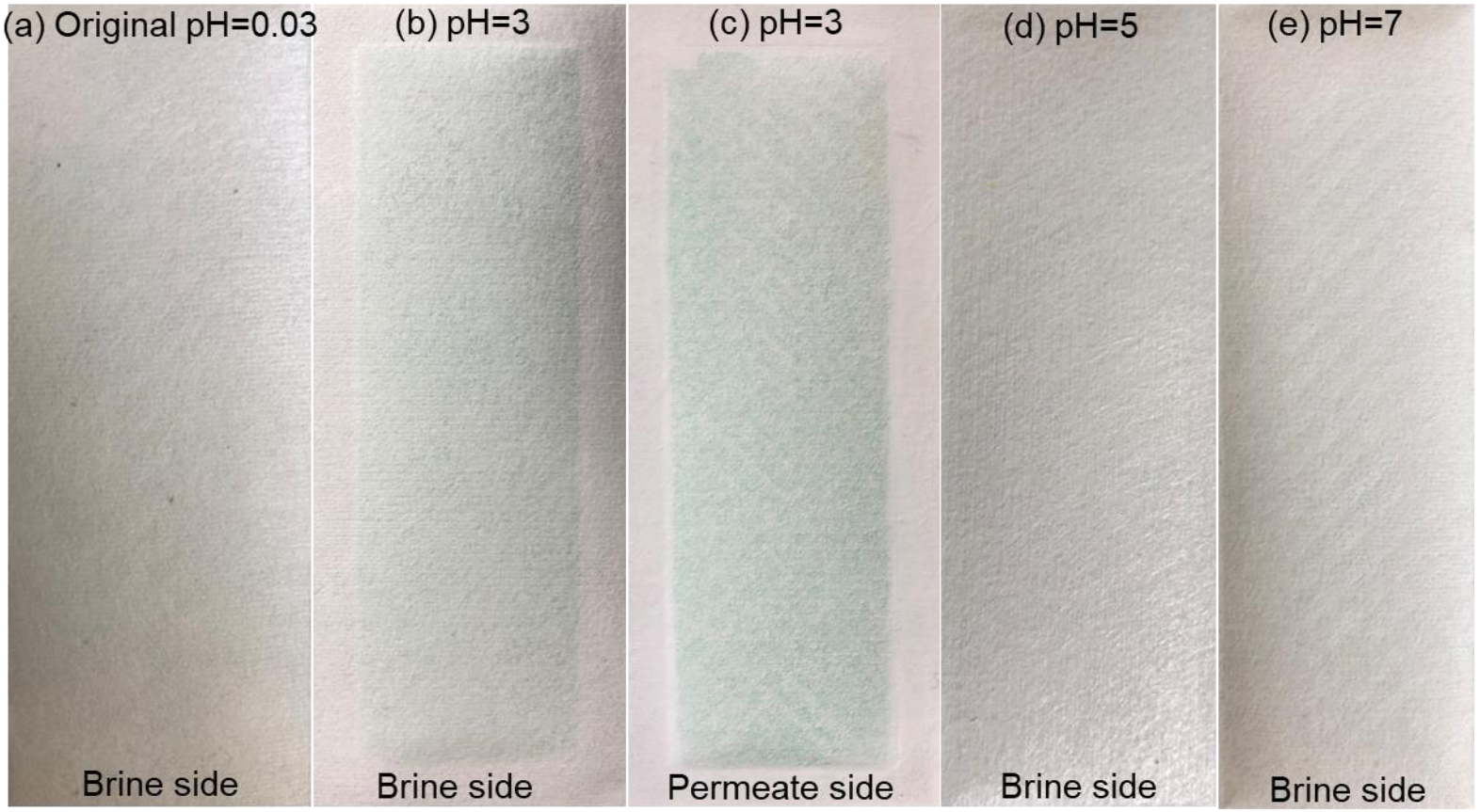

Fig. 3. The photos of brine and permeate sides of PTFE membrane surfaces after experiment under various initial pH of feed solution

.

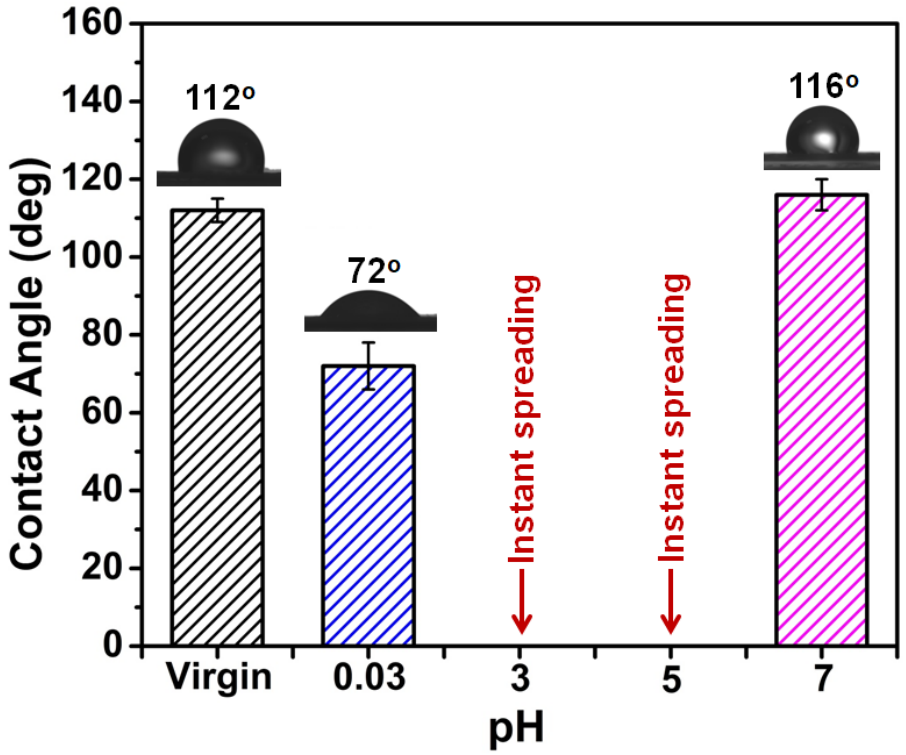

Fig. 4. Contact angle of brine side of PTFE membrane after treatment of refining wastewater with various initial pH.

3.3 Membrane surface morphology

To elucidate the microscopic changes of membrane surface, SEM-EDX has been conducted on each scaled brine side of PTFE membrane surface. As shown in Fig. 5(A), the morphologies of various membrane surfaces were distinct. There is considerable amount of small white particles on the surface fibers of PTFE membrane after treatment of refining wastewater with original pH of 0.03. The corresponding result of EDX (Table 2) showed that the main metallic element was K with ratio of 1.66 wt%, followed by Al (1.32 wt%) and Na (0.94 wt%). Apart from inherent C element of the PTFE membrane, the main non-metallic element was Si with ratio of 42.41 wt%, followed by O (37.53 wt%) and Cl (1.70 wt%). It was reported that Si

286 species in solution with pH less than 9 was mainly in the form of H_4SiO_4 in previous
287 work [44-46]. The polymerization of silica takes place via condensation mechanism in
288 the presence of hydroxide ions. It started with a dimerization reaction that is typically
289 considered to involve a non-ionic silicic acid molecule and an ionic silicic acid
290 molecule (Eqs. (2) - (3)). The dimerization also occurs in an acidic solution but in a
291 much slower rate via the reaction scheme in Eq. (4). Additionally, it was also reported
292 that in the presence of metal ions such as Na^+, Mg^{2+}, Al^{3+}, Ca^{2+} and Fe^{3+}, dimerization
293 was facilitated by neutralizing the surface charge of silica and allow aggregation of
294 particles [47-50]. Based on the analysis from the perspective of elementary
295 composition of scalant and silica polymerization, it can be concluded that the white
296 small scalants deposited on the fibers were possible mixture of mono-silicic acid and
297 silica oligomers.

298 $$H_4SiO_4 + OH^- = H_3SiO_4^- + H_2O \quad (2)$$

299 $$H_3SiO_4^- + H_3SiO_4^- = (OH)_3Si - O - Si(OH)_3 + OH^- \quad (3)$$

300 $$H_4SiO_4 + H_4SiO_4 = (OH)_3Si - O - Si(OH)_3 + H_2O \quad (4)$$

301 However, compared with surface morphology of the PTFE membrane after
302 treatment of refining wastewater with original pH of 0.03, the surface of the PTFE
303 membrane after treatment of refining wastewater with initial pH of 3 was seriously
304 fouled by the evidence that a lot of small spherical particles not only deposited on the
305 surface fibers (Fig. 5(B)), but also aggregated in the gap between the fibers. The
306 corresponding EDX result (Table 2) showed that beside the C element the major
307 non-metallic elements were P, O and Cl with ratio of 26.26 wt%, 24.37 wt% and 5.48

wt%, respectively. The highest content metallic element was Cr with ratio of 17.57 wt%, followed by K (7.66 wt%), Na (5.33 wt%) and Al (5.08 wt%). Based on this result, it can be explained reasonably that the greenish scaled membrane surface showed in Fig. 4 was caused by trivalent chromium (Cr (III)) as the Cr (III) ions in water solution was green [51, 52].

Surface fibers of membrane after treating refining wastewater with initial pH of 5 were relatively clear, large massive scalants were mainly found at the crossing of surface fibers beside few small white particles deposited on the surface fibers (Fig. 5(c)). According to the corresponding EDX results (Table 2), the major non-metallic elements were O (29.69 wt%), Cl (16.77 wt%), P (12.40 wt%), and Si (0.88 wt%). Na was the main metallic element with a ratio of 11.47 wt% followed by Cr (8.76 wt%), K (7.69 wt%) and Al (3.88 wt%). Based on the scalants morphologies and EDX elementary composition analysis, the main scalants was possible a mixture of amorphous silica and silica oligomers.

The surface morphology of PTFE membrane after treatment of neutral (pH=7) refining wastewater looked similar to that of membrane after treatment of original refining wastewater (Fig. 5(D)). EDX result (Table 2) showed that the major non-metallic element was Cl with ratio of 28.49 wt%, followed by O (16.23 wt%), P (5.61 wt%), Si (1.62 wt%) and S (1.06 wt%). The metal elements in the order of content from high to low were Na (13.48 wt%), K (9.23 wt)%, Cr (5.1 wt%), Fe (2.55 wt%) and Al (0.62 wt%). Compared with Si ratio on the membrane surface after treating original refining wastewater, the Si ratio on the membrane surface after

330 treatment of neutral (pH=7) refining wastewater was much lower. The membrane
331 surface morphology was in line with Si ratio on the scaled membrane surface. Only
332 few small white particles were found on surface fibers, resulting in the maximum
333 contact angle the PTFE membrane after experiment.

334 Overall, based on the shape of scalants and their EDX elementary composition
335 analysis, it can be concluded that silica and chromium scaling were occurred on
336 membrane surface. The membrane scaling caused by silica and chromium (III) of the
337 PTFE membrane after treatment of refining wastewater with various initial pH values
338 was in varying degree by evidence that the surface morphologies were distinct, which
339 was possibly the main reason for the changes of DCMD fluxes and contact angles.
340 However, it was noteworthy that silica and chromium scaling occurred and their
341 impacts on system performance were dependent on initial pH of refining wastewater.
342

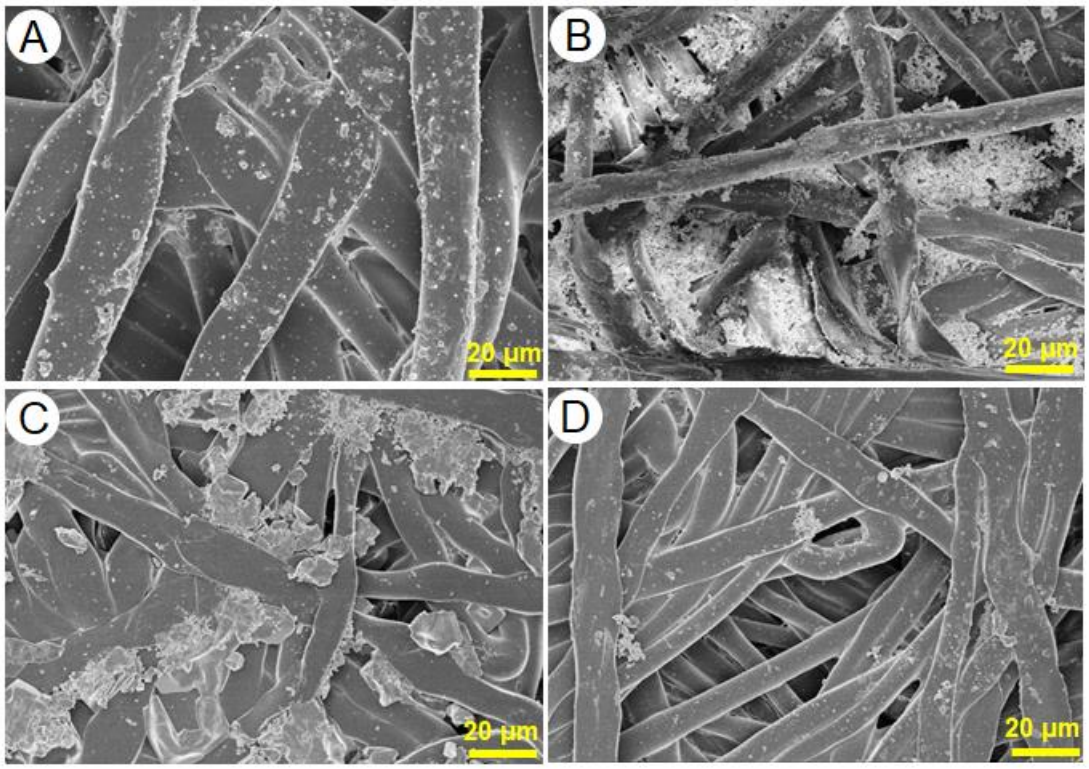

Fig. 5. SEM images of PTFE membrane surface at various initial pH of refining wastewater; (A), (B), (C) and (D) is SEM of scaled membrane treatment of refining wastewater with initial pH of original 0.03, 3, 5 and 7, respectively.

Table 3 The corresponding element ratio of the scaled PTFE membrane surfaces characterized by SEM in Fig. 5

pH	Element ratio (wt%)										
	C	O	Cl	Si	S	P	K	Na	Al	Cr	Fe
0.03	14.44	37.53	1.70	42.41	/	/	1.66	0.94	1.32	/	/
3	8.15	24.37	5.48	/	/	26.26	7.66	5.33	5.08	17.57	/
5	8.46	29.69	16.77	0.88	/	12.4	7.69	11.47	3.88	8.76	/
7	16	16.2	28.5	1.62	1.06	5.61	9.23	13.5	0.62	5.1	2.55

3.4 Mass spectra identified silica oligomers

Mass spectra provided important information of silica oligomers during silica related scaling. The mass spectra of concentrated refining wastewater with various initial pH (Fig. 6) were compared and the mass/charge ration (*m/z*) and possible structure of silica oligomers were tabulated (Table 4). For the concentrated refining wastewater with original pH of 0.03 and 3, the major species in the concentrated solution were mono-silica acid with *m/z* of 113 and dimmer-linear silica acid with *m/z* of 136.9, 155 and 172.9 (Fig. 6 and Table 4). This result indicated that oligomerisation of monomer silica proceeded via formation of dimmer-linear silicates [53-55]. Therefore, the saclants deposited on the PTFE membrane surface was possibly mixture of mono- and dimmer-linear silica acid. The deposition of silica on PTFE membrane is likely to occur via a homogeneous nucleation process, with silica aggregates formed in refining wastewater prior to PTFE membrane surface. The explanation was also consistent with the silica scaling morphology, as distinct silica crystals, especially for original pH of 0.03 (Fig. 5). However, this situation was not for the concentrated refining wastewater with initial pH of 5 and 7. Besides the mono-silica acid with *m/z* of 113 and dimmer-linear silica acid with *m/z* of 155 and 172.9, few trimer-cyclic or –linear and tetramer-cyclic or –linear were also found in the concentrated solution. This phenomenon could be interpreted that mono-silica acid firstly deposited on the PTFE membrane surface and then initiate silica polymerization on the membrane surface, resulting in an amorphous silica scaling morphology, especially for pH of 5.

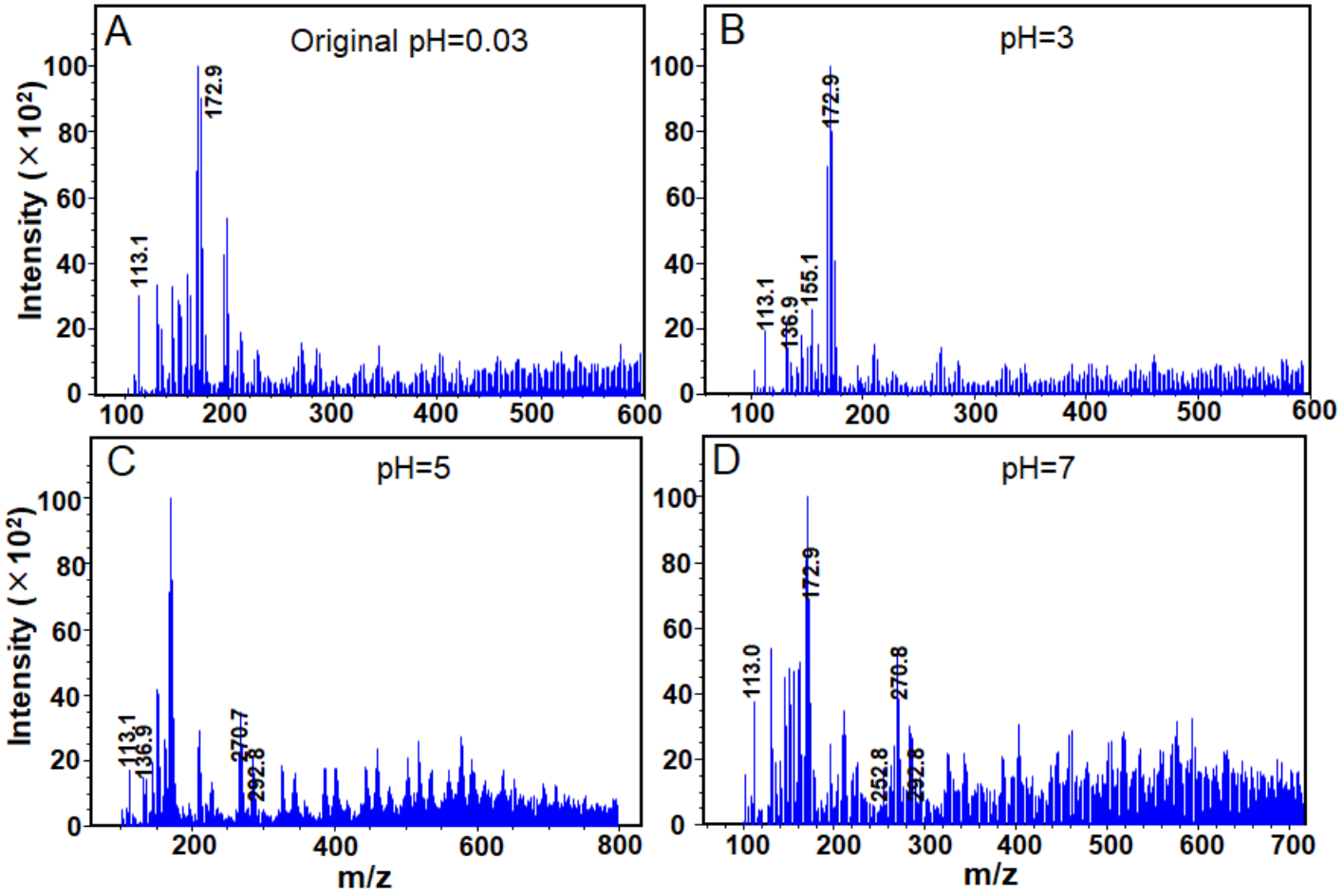

372

373 **Fig. 6.** Mass spectra of the concentrated feed solution with various initial pH after DCMD treatment (A, original pH of 0.03; B, pH=3; C, pH=5;

374 D, pH=7).

375 **Table 4** Possible structures of silica oligomers determined by electrospray ionization mass spectrometry under various initial pH of wastewater.

m/z	Possible molecular formula	Intensity ($\times 10^2$)	Possible structure	Ref
113.1	$H_4SiO_4 \cdot (OH)^-$	30 (original pH) 19 (pH=3) 18 (pH=5) 37 (pH=7)		[53]
136.9	$Si_2O_4(OH)^-$	13 (pH=3) 15 (pH=5)	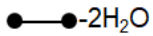	[55]
155.1	$Si_2O_3(OH)_3^-$	26 (pH=3)	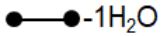	[54]
172.9	$Si_2O_2(OH)_5^-$	90 (original pH) 78 (pH=3) 67 (pH=7)		[53-55]
252.8	$Si_3O_5(OK)(OH)_2^-$	6 (pH=7)	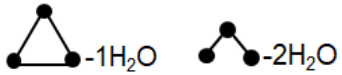	[54]
270.7	$Si_3O_5(OK)(OH)_4^-$	23 (pH=5)		[54]
292.8	$Si_4O_6(OH)_5^-$	7 (pH=5) 7 (pH=7)	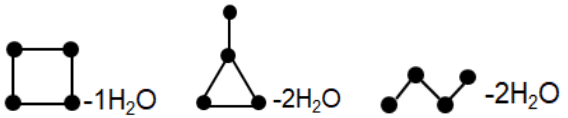	[53, 54]

376

3.5 Chromium (III) scalant identification

Based on the detailed analysis of membrane morphologies and elementary composition from section 3.3, the reason for the scaled PTFE membrane in green under initial pH of 3 was caused by chromium (III). To identify the green species on the scaled membrane surface, the brine side of the scaled PTFE membrane was examined by XPS and UV-Vis spectrophotometer to elucidate the interaction between chromium (III) and membrane and to identify the specific green species.

3.5.1 Chromium (III)-membrane interaction

Based on the results in sections 3.3 chromium (III) scaling was found on the surface of membrane after treating real refining wastewater with initial pH of 3. To elucidate chemical origin of chromium (III)-membrane interaction, high solution XPS was conducted to examine the chemical bond of Cr 2p of the scaled membrane surfaces. The Cr 2p spectra ranging from 568 to 592 eV is shown in Fig. 7. The peaks of Cr 2p binding energy were found at 578.5 eV and 577.4 eV. Based on previous report [56, 57], the peak of Cr 2p binding energy at 578.5 eV and 577.4 eV was the characteristic bond of Cr-Cl and Cr-O, respectively. Further, the intensity of Cr-O was much higher than that of Cr-Cl, indicating that the number of Cr-O was more than that of Cr-Cl in the compounds. According to the analysis above and quality of the real refining wastewater (Table 1), it can be considered that the greenish compounds deposited on the brine side of membrane was chloroaquochromium (III) complexes that was possibly derived from the formation of hydrated isomers of chromic chloride hexahydrate ($CrCl_3 \cdot 6H_2O$) [51, 52]. According to the color of the isomers, the scaled

membrane surface in green was caused by either dichloropentraaquochromiun, $[Cr(H_2O)_5Cl]Cl_2 \cdot H_2O$ or dichlorotetraaquochromiun, $[Cr(H_2O)_4Cl_2]Cl \cdot 2H_2O$.

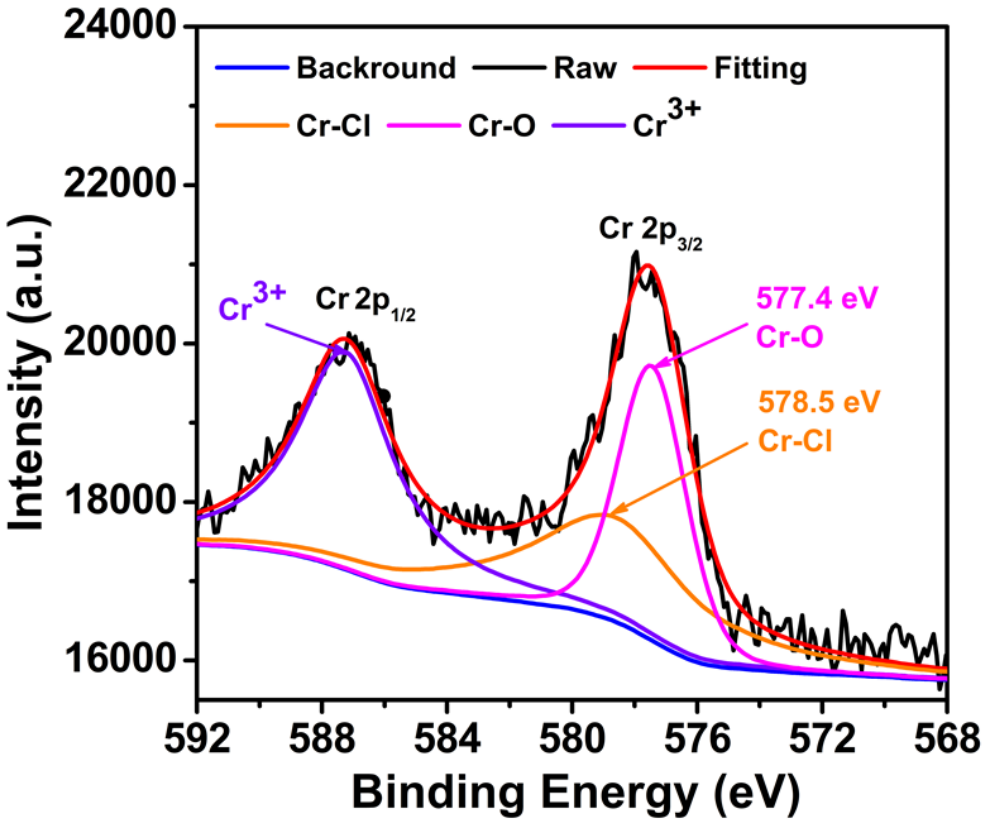

Fig. 7. High solution Cr 2p scan by X-ray photoelectron spectroscopy of scaled membrane after treatment of refining wastewater with various initial pH of 3.

3.5.2 UV-vis absorbance spectra identified dichloroaquochromium (III) complexes

To identify the primary species responsible for the scaled membrane surface in green under condition of feed with initial pH of 3, the test of UV-Vis absorbance of the original and scaled membrane was carried out. In the visible region (380-780 nm), the spectrum of UV-Vis absorbance of the blank membrane was linear (Fig. 8).

412 However, two characteristic peaks at 450 nm and 635 nm with the maximum
413 absorbance value of 0.088 and 0.096, respectively, appeared in the UV-Vis
414 absorbance spectrum of the brine side of the scaled membrane in green. Since
415 previous studies [51, 52, 58] demonstrated that the UV-vis absorption spectrum of
416 $[CrCl_2(H_2O)_4]^+$ showed the characteristic peaks at 450 and 635 nm in the region
417 between 200 and 800 nm, the dichlorotetraaquochromiun, $[Cr(H_2O)_4Cl_2]Cl\cdot 2H_2O$,
418 was the main species responsible for the appeared greenish color. It was reported that
419 the structure of dichlorotetraaquochromiun was octahedral [59]. However, it should be
420 pointed out that the dichlorotetraaquochromiun has two isomeric structures, namely
421 *cis* and *trans* (Fig. 9). Therefore, green specie was possibly mixture of
422 dichlorotetraaquochromium with two isomeric structures.

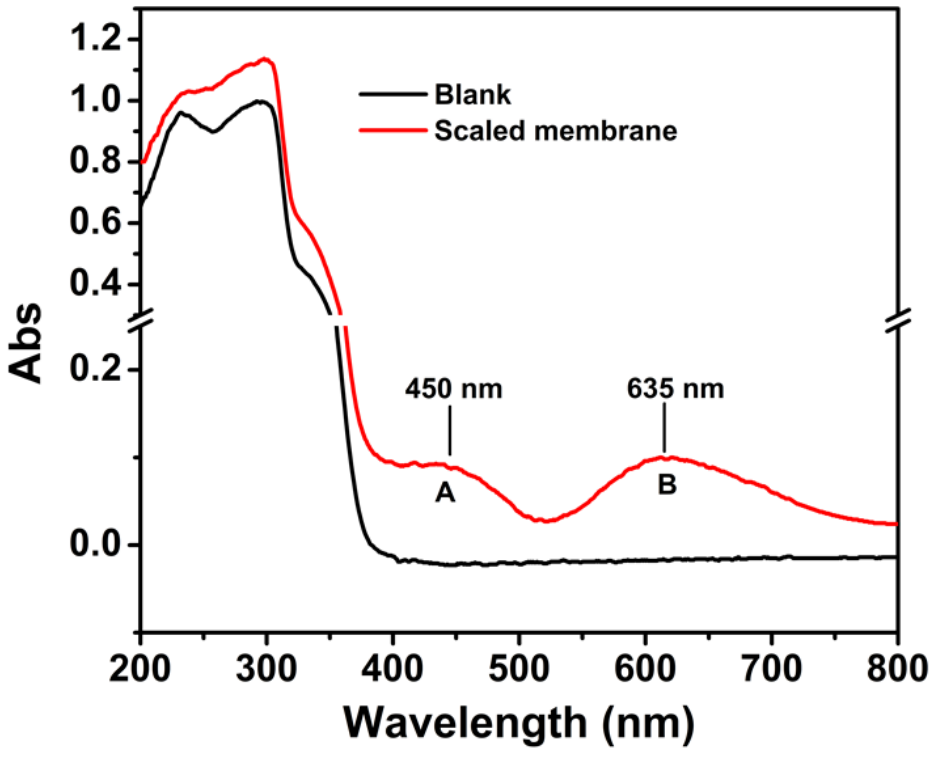

423

424 **Fig. 8.** UV-Vis absorbance spectra of the blank membrane and scaled membrane after
425 treatment of refining wastewater with initial pH of 3.

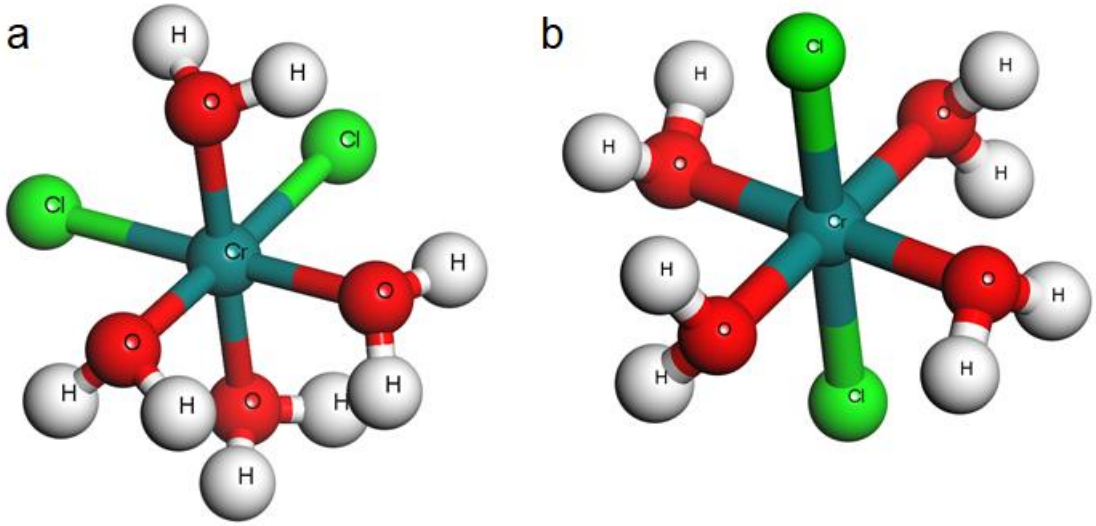

Fig. 9. The molecular space structure of isomeric dichlorotetraaquochromiun (a, *cis*; b, *trans*)

4. Conclusion

In this work, DCMD process was employed to treat real refining wastewater with strong acidity from recovery of precious metals in spent catalysts. System performance was assessed under condition of various initial pH of the real refining wastewater. The major findings and conclusions drawn from this work were summarized as follows.

- High initial water flux ranged from 11.5 to 13 kg/m^{2}h were obtained under various initial pH of refining wastewater as feed through DCMD process.
- Relative pure hydrochloride acid was reclaimed from original refining wastewater through DCMD process.

- High-quality water was available from refining wastewater by adjusting pH from acidic to neutral.
- Silica scaling was the main reason for the decrease of system performance over time when the pH of refining wastewater was adjusted from original 0.03 to 5 and 7.
- Chromium (III) scaling was detected, which resulted in the greenish surfaces of PTFE membrane when the initial pH of refining wastewater was 3. The identified dichlorotetraaquochromiun, $[Cr(H_2O)_4Cl_2]Cl \cdot 2H_2O$, was the main species responsible for the appeared greenish colour.

Acknowledgements

The authors would like to thank the partial financial support from Fundamental Research Funds for the central Universities (No.2232018D3-09, 2232019G-11), Subject construction funds of College of Environmental Science and Engineering and the National Natural Science Foundation of China (No.21507142, 21477018, 51478099), the Natural Science Foundation of Shanghai, China (No. 18ZR1401000), and the Shanghai Pujiang Program (No. 18PJ1400400).

References

[1] H. Dong, J. Zhao, J. Chen, Y. Wu, B. Li, Recovery of platinum group metals from spent catalysts: A review, International Journal of Mineral Processing, 145 (2015) 108-113.

[2] Y. Ding, S. Zhang, B. Liu, H. Zheng, C.-c. Chang, C. Ekberg, Recovery of precious metals from electronic waste and spent catalysts: A review, Resources, Conservation and Recycling, 141 (2019) 284-298.

[3] M.K. Jha, J.-c. Lee, M.-s. Kim, J. Jeong, B.-S. Kim, V. Kumar, Hydrometallurgical recovery/recycling of platinum by the leaching of spent catalysts: A review, Hydrometallurgy, 133 (2013) 23-32.

[4] T.H. Nguyen, C.H. Sonu, M.S. Lee, Separation of Pt(IV), Pd(II), Rh(III) and Ir(IV) from concentrated hydrochloric acid solutions by solvent extraction, Hydrometallurgy, 164 (2016) 71-77.

[5] H.T. Truong, M.S. Lee, G. Senanayake, Separation of Pt(IV), Rh(III) and Fe(III) in acid chloride leach solutions of glass scraps by solvent extraction with various extractants, Hydrometallurgy, 175 (2018) 232-239.

[6] Y. Lu, Z. Xu, Precious metals recovery from waste printed circuit boards: A review for current status and perspective, Resources, Conservation and Recycling, 113 (2016) 28-39.

[7] R. Izatt, S. R Izatt, R. L Bruening, N. E Izatt, B. Moyer, Challenges to Achievement of Metal Sustainability in Our High-Tech Society, Chemical Society reviews, 43 (2014).

[8] H.B. Trinh, J.-c. Lee, R.R. Srivastava, S. Kim, Total recycling of all the components from spent auto-catalyst by NaOH roasting-assisted hydrometallurgical route, Journal of Hazardous Materials, 379 (2019) 120772.

[9] A. Akcil, F. Vegliò, F. Ferella, M.D. Okudan, A. Tuncuk, A review of metal recovery from spent petroleum catalysts and ash, Waste Management, 45 (2015) 420-433.

[10] X. Wei, C. Liu, H. Cao, P. Ning, W. Jin, Z. Yang, H. Wang, Z. Sun, Understanding the Features of PGMs in Spent Ternary Automobile Catalysts for Development of Cleaner Recovery Technology, Journal of Cleaner Production, (2019) 118031.

[11] M.A. Barakat, M.H.H. Mahmoud, Y.S. Mahrous, Recovery and separation of palladium from spent catalyst, Applied Catalysis A: General, 301 (2006) 182-186.

[12] C.A. Kohl, L.P. Gomes, Physical and chemical characterization and recycling potential of desktop computer waste, without screen, Journal of Cleaner Production, 184 (2018) 1041-1051.

[13] G. Gwak, D.I. Kim, S. Hong, New industrial application of forward osmosis (FO): Precious metal recovery from printed circuit board (PCB) plant wastewater, Journal of Membrane Science, 552 (2018) 234-242.

[14] J. Ali, L. Wang, H. Waseem, H.M.A. Sharif, R. Djellabi, C. Zhang, G. Pan, Bioelectrochemical recovery of silver from wastewater with sustainable power generation and its reuse for biofouling mitigation, Journal of Cleaner Production, 235 (2019) 1425-1437.

[15] N. Das, Recovery of precious metals through biosorption — A review, Hydrometallurgy, 103 (2010) 180-189.

[16] S.W. Won, P. Kotte, W. Wei, A. Lim, Y.-S. Yun, Biosorbents for recovery of precious metals, Bioresource Technology, 160 (2014) 203-212.

[17] J.R. Underschultz, S. Vink, A. Garnett, Coal seam gas associated water production in Queensland: Actual vs predicted, Journal of Natural Gas Science and Engineering, 52 (2018) 410-422.

[18] Y. Chun, S.-J. Kim, G.J. Millar, D. Mulcahy, I.S. Kim, L. Zou, Forward osmosis as a pre-treatment for treating coal seam gas associated water: Flux and fouling behaviour, Desalination, 403 (2017) 144-152.

[19] Y. Kim, Y.C. Woo, S. Phuntsho, L.D. Nghiem, H.K. Shon, S. Hong, Evaluation of fertilizer-drawn

503 forward osmosis for coal seam gas reverse osmosis brine treatment and sustainable agricultural reuse,
504 Journal of Membrane Science, 537 (2017) 22-31.
505 [20] G. Chen, Z. Wang, L.D. Nghiem, X.-M. Li, M. Xie, B. Zhao, M. Zhang, J. Song, T. He, Treatment of
506 shale gas drilling flowback fluids (SGDFs) by forward osmosis: Membrane fouling and mitigation,
507 Desalination, 366 (2015) 113-120.
508 [21] B.D. Coday, P. Xu, E.G. Beaudry, J. Herron, K. Lampi, N.T. Hancock, T.Y. Cath, The sweet spot of
509 forward osmosis: Treatment of produced water, drilling wastewater, and other complex and difficult
510 liquid streams, Desalination, 333 (2014) 23-35.
511 [22] K.L. Hickenbottom, N.T. Hancock, N.R. Hutchings, E.W. Appleton, E.G. Beaudry, P. Xu, T.Y. Cath,
512 Forward osmosis treatment of drilling mud and fracturing wastewater from oil and gas operations,
513 Desalination, 312 (2013) 60-66.
514 [23] M.S. Islam, S. Sultana, J.R. McCutcheon, M.S. Rahaman, Treatment of fracking wastewaters via
515 forward osmosis: Evaluation of suitable organic draw solutions, Desalination, 452 (2019) 149-158.
516 [24] S. Kim, M.-H. Song, W. Wei, Y.-S. Yun, Selective biosorption behavior of Escherichia coli biomass
517 toward Pd(II) in Pt(IV)–Pd(II) binary solution, Journal of Hazardous Materials, 283 (2015) 657-662.
518 [25] L. Tan, H. Cui, Y. Xiao, H. Xu, M. Xu, H. Wu, H. Dong, G. Qiu, X. Liu, J. Xie, Enhancement of platinum
519 biosorption by surface-displaying EC20 on Escherichia coli, Ecotoxicology and Environmental Safety,
520 169 (2019) 103-111.
521 [26] H. Xu, L. Tan, H. Cui, M. Xu, Y. Xiao, H. Wu, H. Dong, X. Liu, G. Qiu, J. Xie, Characterization of Pd(II)
522 biosorption in aqueous solution by Shewanella oneidensis MR-1, Journal of Molecular Liquids, 255
523 (2018) 333-340.
524 [27] J. Cui, N. Zhu, N. Kang, C. Ha, C. Shi, P. Wu, Biorecovery mechanism of palladium as nanoparticles
525 by Enterococcus faecalis: From biosorption to bioreduction, Chemical Engineering Journal, 328 (2017)
526 1051-1057.
527 [28] X. Xu, Y. Yang, X. Zhao, H. Zhao, Y. Lu, C. Jiang, D. Shao, J. Shi, Recovery of gold from electronic
528 wastewater by Phomopsis sp. XP-8 and its potential application in the degradation of toxic dyes,
529 Bioresource Technology, 288 (2019) 121610.
530 [29] L.-X. You, D.-M. Pan, N.-J. Chen, W.-F. Lin, Q.-S. Chen, C. Rensing, S.-G. Zhou, Extracellular electron
531 transfer of Enterobacter cloacae SgZ-5T via bi-mediators for the biorecovery of palladium as nanorods,
532 Environment International, 123 (2019) 1-9.
533 [30] X. Ju, K. Igarashi, S.-i. Miyashita, H. Mitsuhashi, K. Inagaki, S.-i. Fujii, H. Sawada, T. Kuwabara, A.
534 Minoda, Effective and selective recovery of gold and palladium ions from metal wastewater using a
535 sulfothermophilic red alga, Galdieria sulphuraria, Bioresource Technology, 211 (2016) 759-764.
536 [31] Y. Jiang, China's water scarcity, Journal of Environmental Management, 90 (2009) 3185-3196.
537 [32] M. Xie, H.K. Shon, S.R. Gray, M. Elimelech, Membrane-based processes for wastewater nutrient
538 recovery: Technology, challenges, and future direction, Water Research, 89 (2016) 210-221.
539 [33] H.C. Duong, F.I. Hai, A. Al-Jubainawi, Z. Ma, T. He, L.D. Nghiem, Liquid desiccant lithium chloride
540 regeneration by membrane distillation for air conditioning, Separation and Purification Technology,
541 177 (2017) 121-128.
542 [34] Y. Chen, R. Zheng, J. Wang, Y. Liu, Y. Wang, X.-M. Li, T. He, Laminated PTFE membranes to enhance
543 the performance in direct contact membrane distillation for high salinity solution, Desalination, 424
544 (2017) 140-148.
545 [35] R. Schwantes, L. Bauer, K. Chavan, D. Dücker, C. Felsmann, J. Pfafferott, Air gap membrane
546 distillation for hypersaline brine concentration: Operational analysis of a full-scale module–New

547 strategies for wetting mitigation, Desalination, 444 (2018) 13-25.
548 [36] G. G, A. G, I. Af, Perspective of renewable desalination by using membrane distillation, Chemical
549 Engineering Research and Design, 144 (2019) 520-537.
550 [37] C.M. Tun, A.G. Fane, J.T. Matheickal, R. Sheikholeslami, Membrane distillation crystallization of
551 concentrated salts—flux and crystal formation, Journal of Membrane Science, 257 (2005) 144-155.
552 [38] N. Dow, S. Gray, J.-d. Li, J. Zhang, E. Ostarcevic, A. Liubinas, P. Atherton, G. Roeszler, A. Gibbs, M.
553 Duke, Pilot trial of membrane distillation driven by low grade waste heat: Membrane fouling and
554 energy assessment, Desalination, 391 (2016) 30-42.
555 [39] M. Morciano, M. Fasano, L. Bergamasco, A. Albiero, M. Lo Curzio, P. Asinari, E. Chiavazzo,
556 Sustainable freshwater production using passive membrane distillation and waste heat recovery from
557 portable generator sets, Applied Energy, 258 (2020) 114086.
558 [40] R. Schwantes, A. Cipollina, F. Gross, J. Koschikowski, D. Pfeifle, M. Rolletschek, V. Subiela,
559 Membrane distillation: Solar and waste heat driven demonstration plants for desalination,
560 Desalination, 323 (2013) 93-106.
561 [41] Z. Xiao, Z. Li, H. Guo, Y. Liu, Y. Wang, H. Yin, X. Li, J. Song, L.D. Nghiem, T. He, Scaling mitigation in
562 membrane distillation: From superhydrophobic to slippery, Desalination, 466 (2019) 36-43.
563 [42] C. Yang, X.-M. Li, J. Gilron, D.-f. Kong, Y. Yin, Y. Oren, C. Linder, T. He, CF4 plasma-modified
564 superhydrophobic PVDF membranes for direct contact membrane distillation, Journal of Membrane
565 Science, 456 (2014) 155-161.
566 [43] M. Tian, Y. Yin, C. Yang, B. Zhao, J. Song, J. Liu, X.-M. Li, T. He, CF4 plasma modified highly
567 interconnective porous polysulfone membranes for direct contact membrane distillation (DCMD),
568 Desalination, 369 (2015) 105-114.
569 [44] S. Sjöberg, Silica in aqueous environments, Journal of Non-Crystalline Solids, 196 (1996) 51-57.
570 [45] Y.-N. Wang, X. Li, R. Wang, Silica scaling and scaling control in pressure retarded osmosis
571 processes, Journal of Membrane Science, 541 (2017) 73-84.
572 [46] N.A. Milne, T. O'Reilly, P. Sanciolo, E. Ostarcevic, M. Beighton, K. Taylor, M. Mullett, A.J. Tarquin,
573 S.R. Gray, Chemistry of silica scale mitigation for RO desalination with particular reference to remote
574 operations, Water Research, 65 (2014) 107-133.
575 [47] W. Zhong, H. Li, Y. Ye, V. Chen, Evaluation of silica fouling for coal seam gas produced water in a
576 submerged vacuum membrane distillation system, Desalination, 393 (2016) 52-64.
577 [48] R. Sheikholeslami, I.S. Al-Mutaz, T. Koo, A. Young, Pretreatment and the effect of cations and
578 anions on prevention of silica fouling, Desalination, 139 (2001) 83-95.
579 [49] T. Koo, Y.J. Lee, R. Sheikholeslami, Silica fouling and cleaning of reverse osmosis membranes,
580 Desalination, 139 (2001) 43-56.
581 [50] S. Salvador Cob, B. Hofs, C. Maffezzoni, J. Adamus, W.G. Siegers, E.R. Cornelissen, F.E. Genceli
582 Güner, G.J. Witkamp, Silica removal to prevent silica scaling in reverse osmosis membranes,
583 Desalination, 344 (2014) 137-143.
584 [51] S. Díaz-Moreno, A. Muñoz-Páez, J.M. Martínez, R.R. Pappalardo, E.S. Marcos, EXAFS Investigation
585 of Inner- and Outer-Sphere Chloroaquo Complexes of Cr3+ in Aqueous Solutions, Journal of the
586 American Chemical Society, 118 (1996) 12654-12664.
587 [52] P.J. Elving, B. Zemel, Absorption in the Ultraviolet and Visible Regions of Chloroaquochromium(III)
588 Ions in Acid Media, Journal of the American Chemical Society, 79 (1957) 1281-1285.
589 [53] M. Xie, S.R. Gray, Silica scaling in forward osmosis: From solution to membrane interface, Water
590 Research, 108 (2017) 232-239.

591 [54] M.E. Simonsen, E.G. Søgaard, ESI-MS investigation of the polymerization of inorganic polymers,
592 International Journal of Mass Spectrometry, 285 (2009) 78-85.
593 [55] P. Bussian, F. Sobott, B. Brutschy, W. Schrader, F. Schüth, Speciation in Solution: Silicate Oligomers
594 in Aqueous Solutions Detected by Mass Spectrometry, Angewandte Chemie International Edition, 39
595 (2000) 3901-3905.
596 [56] Y. Qi, M. Jiang, Y.-L. Cui, L. Zhao, S. Liu, Novel reduction of Cr(VI) from wastewater using a naturally
597 derived microcapsule loaded with rutin–Cr(III) complex, Journal of Hazardous Materials, 285 (2015)
598 336-345.
599 [57] M.C. Biesinger, C. Brown, J.R. Mycroft, R.D. Davidson, N.S. McIntyre, X-ray photoelectron
600 spectroscopy studies of chromium compounds, Surface and Interface Analysis, 36 (2004) 1550-1563.
601 [58] C.W. Merideth, W.D. Mathews, E.F. Orlemann, The Rate of Aquation of Dichlorotetraaquochromic
602 Ion as a Function of pH in Chloride Media, Inorganic Chemistry, 3 (1964) 320-322.
603 [59] B. Morosin, The crystal structure of [Cr(H2O)4Cl2]Cl.2H2O, Acta Crystallographica, 21 (1966)
604 280-284.
605